Distribution and motions of atomic hydrogen in lenticular galaxies. X. The blue SO galaxy NGC 5102

van Woerden, H; van Driel, W; Braun, R; Rots, AH

Published in:
Astronomy & astrophysics

Astron. Astrophys. 269, 15–28 (1993)

ASTRONOMY AND ASTROPHYSICS

Distribution and motions of atomic hydrogen in lenticular galaxies*

X. The blue S0 galaxy NGC 5102

H. van Woerden[1], **W. van Driel**[1,2,3], **R. Braun**[4,5], **and A.H. Rots**[4,6]

[1] Kapteyn Astronomical Institute, Groningen University, Postbus 800, NL-9700 AV Groningen, The Netherlands
[2] Observatoire de Paris, Section de Meudon, DAEC, UA 173, Laboratoire d'Astrophysique associé à l'Université de Paris VII, F-92195 Meudon principal Cedex, France
[3] Astronomical Institute "Anton Pannekoek", University of Amsterdam, Kruislaan 403, NL-1098 SJ Amsterdam, The Netherlands
[4] National Radio Astronomical Observatory, P.O. Box 0, Socorro NM 87801, U.S.A.
[5] Radiosterrewacht Dwingeloo, Postbus 2, NL-7990 AA Dwingeloo, The Netherlands
[6] Present address: NASA Goddard Space Flight Center, Code 666, Greenbelt, MD 20771, USA

Received June 28, accepted October 17, 1992

Abstract. We have mapped the blue gas-rich S0 galaxy NGC 5102 in the 21-cm HI line with a spatial resolution of $34'' \times 37''$ ($\Delta\alpha \times \Delta\delta$) and a velocity resolution of 12 km s^{-1}. Optically NGC 5102 is a peculiar S0 galaxy, in the sense that it has unusually blue colours, and shows evidence for a burst of star formation a few times 10^8 years ago in its nucleus. Also the inner bulge and parts of its disk show signs of low-level star formation activity. It further has a 'supershell' of 1.7 kpc diameter seen in Hα around its central regions, a unique feature for a lenticular galaxy.

The HI distribution has a pronounced central depression of 1.9 kpc radius, and most of the HI is concentrated in a 3.6 kpc wide ring with an average radius of 3.7 kpc (= 0.7 R_{25}), assuming a distance of 4 Mpc for NGC 5102. The maximum azimuthally averaged HI surface density in the ring is 1.4 $M_\odot$ pc^{-2}, comparable to that found in other S0 galaxies. The extent of the HI gas is not much larger than the optical de Vaucouleurs' radius (R_{25}) of the galaxy, contrary to what is found in other gas-rich S0's, which often have large outer HI rings at R $\sim$ 2 R_{25}. The HI velocity field is quite regular, showing no evidence for large-scale deviations from circular rotation, and the HI is found to rotate in the plane of the stellar disk. The rotation curve is essentially flat at $V_{rot} \sim 95$ km s^{-1} out to R = 6 kpc (1.1 R_{25}). Assuming a simple spherical mass model, we find a total mass-to-light ratio $M_T/L_B^0 = 4.3\ M_\odot/L_\odot$ within R = 6 kpc.

In contrast to other S0 galaxies studied in this series of papers, both the HI mass/blue luminosity ratio and the radial HI distribution are similar to those in early-type spirals. The HI may be an old, "smouldering", disk or it may have been acquired through capture of a gas-rich smaller galaxy. The recent starburst in the nuclear region, which gave the galaxy its blue colour, may have been caused by partial radial collapse of the gas disk, or by infall of a gas-rich dwarf galaxy.

Key words: galaxies: kinematics and dynamics of – galaxies: lenticular – galaxies: structure of – galaxies: individual: NGC 5102

1. Introduction

This paper is one in a series presenting the results of studies of lenticular (or, equivalently, S0) and other early-type disk galaxies, using 21-cm HI observations obtained with the Westerbork Synthesis Radio Telescope (WSRT) or the Very Large Array (VLA). These studies aim at an understanding of the origin and evolution of the gaseous component in gas-rich lenticular galaxies, through a determination of the distribution and motions of HI in these systems. While for spiral galaxies the hydrogen content, expressed in terms of the M_{HI}/L_B ratio, increases smoothly from the early to the late types (e.g. Shostak 1978; Bottinelli et al. 1980), lenticular galaxies show a very wide range of measured M_{HI}/L_B-ratios ($\sim$0.0005–0.7 $M_\odot/L_\odot$), suggesting that their HI content is not related to their stellar component (Wardle & Knapp 1986; Roberts et al. 1991).

With the WSRT or the VLA we have mapped the HI distribution and motions in (and around) 11 S0, 6 S0/a, 3 S0? and

Send offprint requests to: Hugo van Woerden

* The National Radio Astronomical Observatory is operated by Associated Universities, Inc., under contract with the U.S. National Science Foundation

S0pec, and 3 Sa-type galaxies which have good single-dish detections: NGC 1291, 3619, 3626, 3900, 3941, 3998, 4026 and companions, 4203, 4262, 4694, 5101, 6500/6501 and 7013, and IC 5267 (see papers I to IX, and XI: van Woerden et al. 1983; Knapp et al. 1984, 1985; Krumm et al. 1985; van Driel et al. 1988a, 1988b, 1988c, 1989; van Driel & van Woerden 1989, 1991; see also van Driel 1987). In the present paper, VLA observations of the southern S0 galaxy NGC 5102 are presented.

NGC 5102 is of particular interest to our study of gas-rich lenticulars, as it is a morphologically pure S0 with a blue nuclear region, showing signs of recent star formation activity (see Sect. 2). Also, it is one of the nearest S0's, and its optical luminosity ($L_B^0 = 2.8 \times 10^9\ L_\odot$, comparable to galaxies like M33) is smaller than that of the other lenticulars discussed in this series of papers.

The systemic heliocentric radial velocity of NGC 5102 is 470 km s^{-1} (see Sect. 4.3). Since it is probably a member of the nearby NGC 5128 group, we adopt for NGC 5102 the distance to this group derived by de Vaucouleurs (1975), and de Vaucouleurs & Olson (1984), i.e. 4 Mpc. Jacoby et al. (1988), using planetary nebulae as distance indicators, find 3.8±0.2 Mpc for NGC 5128.

The organization of this paper is as follows. In the next section the optical, X-ray, and infrared properties of NGC 5102 are summarized. In Sect. 3 the HI synthesis observations are described and in Sect. 4 the HI distribution and rotation curve are presented. In Sect. 5 the results are discussed and in Sect. 6 we present our conclusions.

2. Optical, X-ray and infrared properties

The optical, X-ray and infrared properties of NGC 5102 are summarized in Table 1, together with other integral properties (but excluding those derived from the 21-cm line observations).

Note that the velocities in this paper, unless otherwise indicated, are heliocentric and calculated according to the conventional optical definition ($V = c\Delta\lambda/\lambda_0$).

2.1. Optical, UV and X-ray properties

A blue photograph of NGC 5102 is shown in Fig. 1; other photographs of the galaxy, taken with larger telescopes, have been published by van den Bergh (1976), and by Danks et al. (1979). NGC 5102 has been classified as $S0_1$ by Sandage & Tammann (1981, hereafter RSA), as $SA0^-$ by de Vaucouleurs et al. (1976, RC2), and as S0 by Lauberts (1982, EUS). NGC 5102 has been listed as a member of de Vaucouleurs' (1975) group G4.

Surface photometry of NGC 5102 has been published by Burstein et al. (1987), Evans (1952), Pritchet (1979), Sérsic (1968), and Williams & Schwarzschild (1979), and has been made available to us by Lauberts & Valentijn (1985, 1989, and private communication). The average radial distributions of light and colour in the galaxy are illustrated in Fig. 2. The luminosity profile shows the presence of a nucleus, bulge, and exponential disk, confirming the S0-classification. As indicated in Fig. 2, we have derived photometric parameters of the bulge

Table 1. Optical and infrared properties of NGC 5102

R.A. (1950.0)	$13^h19^m07^s$	RC2
Dec. (1950.0)	$-36°22'06''$	RC2
Morphological type	$S0_1$	RC2
	$SA0^-$	RSA
	S0	EUS
Assumed distance	4.0 Mpc	*
Optical diameter D_0	8.′5	RC2
	9.9 kpc	*
Optical diameter D_{25}	9.′3	RC2
Disk centr. brightn. $\mu_B(0)$	22.2 mag/arcsec^2	*
Disk scalelength	1.7 kpc	*
Bulge eff. radius	0.26 kpc	*
Disk/bulge lumin. ratio	4.5	*
Inclination (opt.)	71°	RC2
Inclination (HI)	70°	*
Maj. axis pos. angle (opt.)	48°	EUS
Maj. axis pos. angle (HI)	43°	*
B_T^0	9.86 mag	RC2
$(B-V)_T^0$	0.58 mag	RC2
$(U-B)_T^0$	0.19 mag	RC2
Syst. helioc. veloc.	470 km s^{-1}	*
Blue luminosity L_B^0	$2.8 \times 10^9\ L_\odot$	*
$\log(L_{FIR}/L_B^0)$	−2.0	R,*
$\log(S_{100\mu}/S_{60\mu})$	0.49	R
L_X/L_B^0 (0.5–4.5 keV)	$< 3 \times 10^{-5}$	FJT
centr. stellar vel. disp.	145 km s^{-1}	FJ

References: EUS: Lauberts (1982), FJ: Faber & Jackson (1976), FJT: Forman et al. (1985), R: Rice et al. (1988), RC2: de Vaucouleurs et al. (1976), RSA: Sandage & Tammann (1981), *: this paper

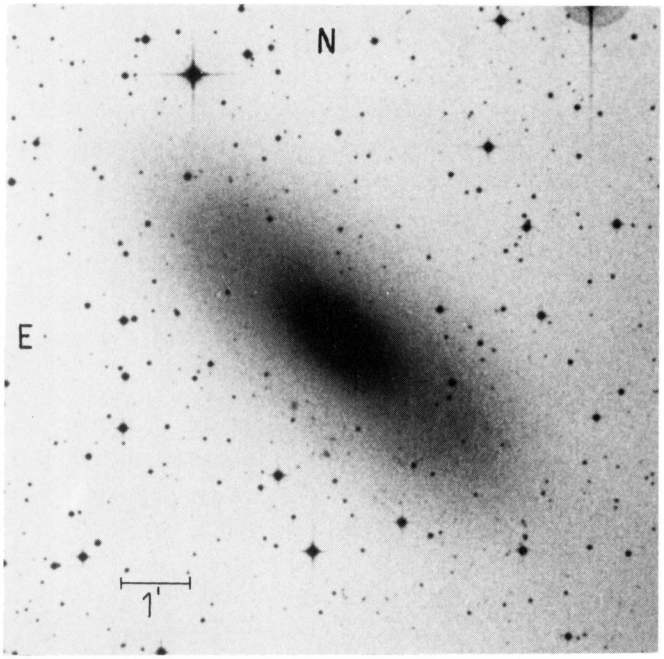

Fig. 1. NGC 5102, from a blue ESO/SRC sky survey copy. The glare to the west of the galaxy is caused by a bright star

and disk from this profile, following Burstein's (1979) decomposition method. We find a disk scalelength r_0 = 1.′5 = 1.7 kpc, a central disk surface brightness, corrected for galactic absorption and inclination, of $\mu_B(0)$ = 22.2 mag arcsec^{-2}, an effective bulge radius r_e = 0.′22 = 0.26 kpc, and a disk-to-bulge luminosity ratio D/B = 4.5; the De Vaucouleurs diameter D_{25} is 9.′3 = 10.8 kpc. Simien & de Vaucouleurs (1986), and Yoshizawa and Wakamatsu (1975) derive different photometric parameters for NGC 5102, using Sérsic's (1968) profile. We prefer to use the more recent results of Lauberts & Valentijn. At small radii (R < 10″) the galaxy shows a small isophotal twist, and the isophotes become rounder towards the centre. This may be caused by obscuring dust, or by triaxiality of the bulge (Pritchet 1979).

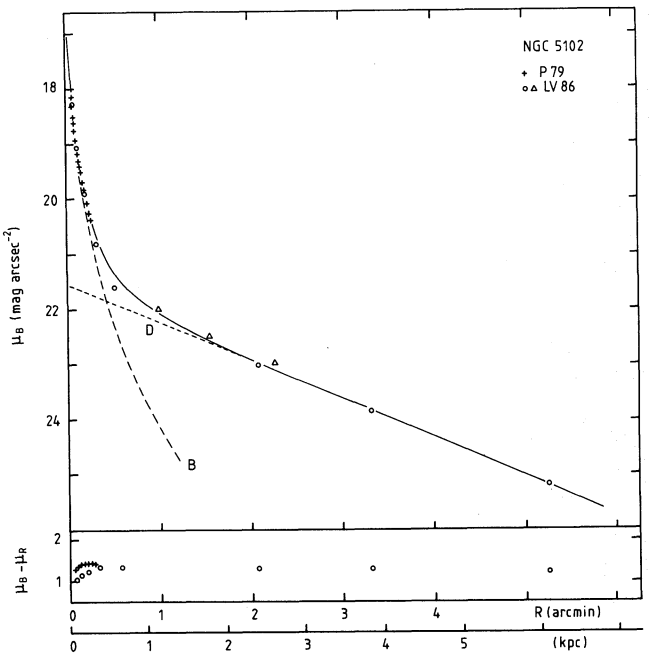

Fig. 2. Azimuthally averaged radial surface brightness distribution of NGC 5102 in the B-band, μ_B(R), and of the ($\mu_B - \mu_R$) colour (*P79*: Pritchet, 1979, *LV 86*: Lauberts and Valentijn, private communication, **o** derived using fixed inclination and major axis position angle, and Δ using fitted inclinations and position angles). An exponential disk (*D*) and a bulge (*B*) have been fitted to the profile, as explained in the text

The blue colour of NGC 5102 was first noted by Freeman (see Eggen 1971). The integrated colours of the galaxy, $(B-V)^0_T$ = 0.58 mag and $(U-B)^0_T$ = 0.19 mag (RC2), are bluer than that of a typical lenticular. As may be seen in Fig. 2, NGC 5102 has a clear colour-gradient in the inner region (R < 20″), the inner part being bluer. Pritchet (1979) detected a bright, small, blue nucleus in NGC 5102. The nucleus has a diameter < 1″ (= 20 pc), a blue magnitude −14, hence $L_B = 6 \times 10^7$ $L_\odot$, and $(B-V)_0$ = 0.2±0.1 mag, distinctly much bluer than the surrounding bulge, which has $(B-V)_0$ = 0.7 mag. The colours of the nucleus are consistent with a burst of star formation a few times 10^8 years ago (Glass & Moorwood 1984; Pritchet 1979; van den Bergh 1976). The inner bulge also shows evidence for some recent star formation activity.

On large-scale plates and CCD images of NGC 5102 (van den Bergh 1976; Danks et al. 1979; Danks, private communication) various (small-scale) structures can be seen in the galaxy. (*1.*) An 11″ long Hα filament emerging from the central region, which however is only the brightest part of a 'supershell' of about 1.′5 (1.7 kpc) diameter seen on deeper Hα CCD images (Ciardullo et al. 1988; Jacoby, private communication). The supershell is quite asymmetric. Its brightest part lies close to the nucleus on its SE side. Fainter parts reach distances of 0.′8 on the ENE and WSW sides and 1.′1 towards the NNW. Fabry-Perot images (Ciardullo, private communication) show that the spectral lines in this supershell are quite narrow (<50 km s^{-1}), indicating that the shell is probably not shock-ionized. Most of the shell has negative velocities relative to the systemic velocity (Jacoby, private communication). (*2.*) Dust lanes parallel to the major axis, with position angles of 200° to 240°, at R = 3″ − 16″ (Danks et al. 1979). (*3.*) A "sprinkling of faint stars across the disk" (Van den Bergh 1976), of B ∼ 22 mag or $M_B \sim -6.5$ mag, probably blue supergiants or young open clusters, with ages $\leq 3 \times 10^7$ years. Two of the most prominent groupings, 1.′1 south-east and 1.′6 south of the nucleus (i.e. at radial distances R in the plane of R = 3.′1 = 3.6 kpc and 3.′8 = 4.4 kpc), are embedded in diffuse HII regions of 8″ − 13″ diameter (Van den Bergh 1976). (*4.*) Numerous dust patches in the disk, especially in the south-western part, of 2″ − 10″ diameter. The total estimated dust mass is ∼10^4 $M_\odot$ (Danks et al. 1979; cf. Sect. 2.2.).

Optical spectra of NGC 5102 have been discussed by Alloin & Bica (1989), Balkowski et al. (1986), Bica & Alloin (1987a, 1987b, 1987c), Bica (1988), Bonatto et al. (1989), Davies et al. (1987), de Vaucouleurs & de Vaucouleurs (1967), Evans (1963), and Gallagher et al. (1975); near-infrared spectra by Moorwood & Oliva (1988), and far-ultraviolet spectra by Burstein et al. (1988), Miller & Wu (1984), Rocca-Volmerange & Balkowski (1984), & Rocca-Volmerange & Guiderdoni (1987). NGC 5102 has only weak Hα and [N II]emission lines and no near-infrared emission lines were found. The optical nuclear spectrum shows quite weak emission lines, and is dominated by A-type stars (Gallagher et al. 1975), like in NGC 4694 (van Driel & van Woerden 1989). The IUE far-UV spectra show the presence of a population of A-type stars, plus some OB stars, consistent with the idea of a starburst some 3 × 10^8 years ago plus some recent star formation. The population synthesis studies of Bica & Alloin (see references above) indicate that the metallicity of NGC 5102 is sub-solar, $[Z/Z_\odot] \sim -0.5$, and consistent with its moderate luminosity.

No X-ray emission was detected from NGC 5102 with the Einstein Observatory in the 0.5–4.5 keV region, giving $L_X < 3.3 \times 10^{38}$ erg s^{-1}, and $L_X/L_B < 3.0 \times 10^{-5}$; these are low values for a field S0 (Canizares et al. 1987; Fabbiano et al. 1989; Forman et al. 1985; Trinchieri & Fabbiano 1985), but of course NGC 5102 is a low-luminosity object.

Central stellar velocity dispersions σ_* of 145 and 66 km s^{-1} were measured in NGC 5102 by, respectively, Faber & Jackson

(1976), and Davies et al. (1987); a value of about 150 km s^{-1} would be normal for an S0 of its moderate luminosity (Dressler and Sandage 1983).

In summary, the S0 galaxy NGC 5102 shows evidence for a burst of star formation some 10^8 years ago in its nucleus, and for (some) recent star formation throughout its bulge and disk. The global morphology of its light distribution is normal for an S0, but the 'supershell' of 1.7 kpc diameter seen in Hα is a unique feature for a lenticular galaxy.

2.2. Infrared properties

Photometry and spectra of NGC 5102 in the near-infrared (Persson et al. 1979; Glass & Moorwood 1984; Bica & Alloin 1987b) also indicate a recent burst of star formation in its inner region. Far-infrared emission from NGC 5102 has been detected in all four IRAS bands (Knapp et al. 1989; Lonsdale et al. 1985 and 1989; Rice et al. 1988). From the ratio of 60 and 100 μm flux densities of Knapp et al. (1989) we derive an average dust temperature of T_d = 33 K, assuming a λ^{-1} dust emissivity law and a single-temperature dust distribution. We also estimated a far-infrared luminosity, L_{FIR}, based on the far-infrared flux parameter FIR (see Lonsdale et al. 1985; Helou et al. 1989). We find $L_{FIR} = 4.9 \times 10^7$ $L_\odot$, and $\log(L_{FIR}/L_B^0) = -1.76$ for NGC 5102.

NGC 5102 was also observed twice at 50 and 100 μm with the CPC detectors of IRAS (see Wesselius et al. 1985; Wainscoat et al. 1987), but it was not detected, since this detector has a lower sensitivity than the Survey Instrument.

Compared to a sample of detected SO galaxies from the RSA (van Driel & de Jong 1990), NGC 5102 has a normal dust temperature, but low L_{FIR}/L_B^0 and M_d/L_B^0 ratios for its $S0_1$ classification, despite the presence of dust lanes and patches. If we interpret the relationship between dust temperature and L_{FIR}/L_B-ratio in terms of star formation activity (cf. de Jong et al. 1984; de Jong & Brink 1987), then NGC 5102, at present, has a quite low global star formation rate, even compared to other lenticulars.

Adopting a far-infrared dust opacity (Gillett et al. 1988) of $\kappa_0 = 2.3 \times 10^4$ cm^2 gr^{-1} at 100 μm, and using a single-temperature dust distribution, we would estimate a radiating dust mass from the IRAS 60 and 100 μm data of $M_d = 1.5 \times 10^3$ $M_\odot$, a value lower than the optical estimate of 10^4 $M_\odot$ of Danks et al. (1979, see Sect. 2.1.). Note that the HI gas-to-dust mass ratio in NGC 5102 derived in this way, $\sim 10^5$, is about three orders of magnitude higher than the canonical Galactic value of about 150 (see e.g. Spitzer 1978).

However, various authors (e.g. de Jong & Brink 1987) have proposed simple two-component dust models for galaxies, with a warm dust component of some 60 K temperature imbedded in the star forming regions and a cool component of some 16–20 K associated with the general interstellar radiation field. The application of such a model with cool dust of 18 K (van den Broek 1990, 1992; van Driel and van den Broek 1991) to NGC 5102 indicates that we would underestimate the actual radiating dust mass by about a factor of 35, if we assume a single-temperature dust distribution (like we did above), since most of the dust radiates at wavelengths longwards of the IRAS limit at $\lambda > 120$ μm. Note, however, that this factor is critically dependent on the cool-dust temperature; it would be about 150 for 16 K and only 8 for 20 K.

3. VLA 21-cm line observations

We reduced and analyzed 21-cm HI line observations of NGC 5102 which were obtained with the Very Large Array (VLA) radio synthesis telescope in 1983 by N. Thonnard and F. Schweizer, and made available to us in 1986. A summary of observational and instrumental parameters is given in Table 2. The VLA synthesis telescope and the general method of spectral-line data handling have been described by Hjellming (1983) and Rots (1982). All data handling at the VLA site was performed using standard VLA software. The data were calibrated using standard VLA continuum sources. A digital spectrometer was used to obtain data simultaneously in 31 frequency channels. The velocity resolution is 12 km s^{-1}, 1.2 times the channel separation. The data were edited and Fourier-transformed, resulting in maps of the brightness distribution in each velocity channel. These maps have a HPBW spatial resolution of $34'' \times 37''$ ($\Delta\alpha \times \Delta\delta$). The final data processing was carried out with the interactive Groningen Image Processing System, GIPSY (Allen et al. 1985).

Table 2. Instrumental parameters for HI observations

Observing dates	8,9 Jan 1983
Total observing time	12 hrs
VLA configuration[a]	C/D array
Field centre (R.A.) (1950.0)	$13^h19^m07^s$
(Dec.) (1950.0)	$-36°22'06''$
Synthesized HPBW ($\alpha \times \delta$)	$34'' \times 37''$
Primary beam	$31'$
Central rad. vel.	468 km s^{-1}
Total bandwidth	1.56 MHz
Channel separation	10.3 km s^{-1}
Velocity resolution	12.3 km s^{-1}
rms noise in channel maps	2.0 mJy/beam
	0.97 K

Notes: a: NS arm in C-array, others in D-array

4. Results

4.1. Radio continuum

Averaging the line-free channels at both ends of the band, we have made a CLEANed map of the 21-cm continuum emission. This map, which has a noise of 0.3 mJy/beam, shows no extended emission but two compact sources: a nuclear source of S = 1.9±0.5 mJy, and a source of S = 8.3±0.6 mJy at $\alpha = 13^h19^m18^s.56 \pm 0^s.04$, $\delta = -36°21'31''.3 \pm 0''.5$, i.e. 39″

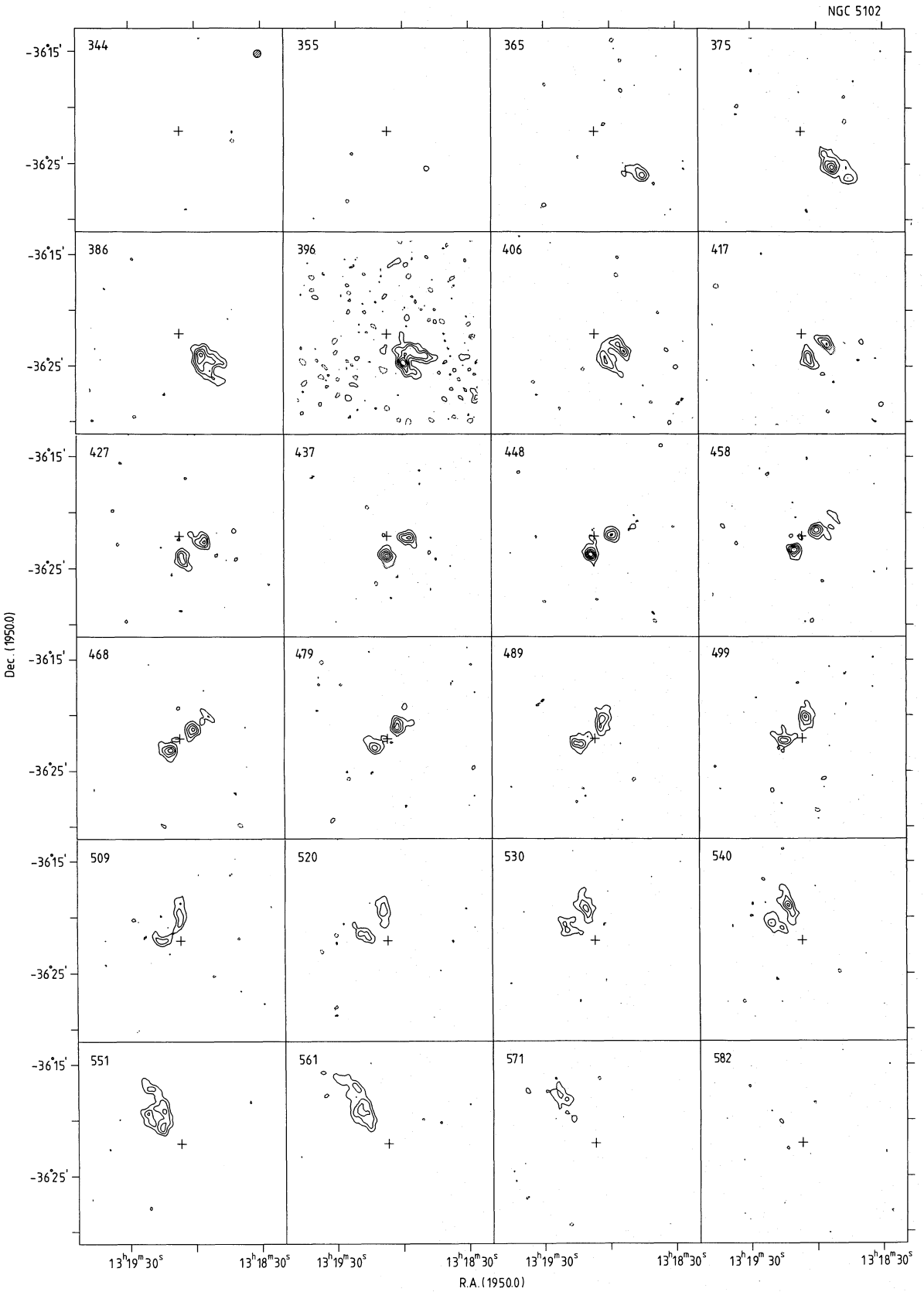

Fig. 3. Channel maps of NGC 5102, with a resolution (HPBW) of $34'' \times 37''$ ($\alpha \times \delta$), indicated by the hatched ellipse in the top left panel. The velocity of each map is shown in its upper left-hand corner. Contours are $T_b = -2.9$, 2.9, 5.8, 8.7, 11.6, and 14.5 K; negative contours are dashed. The rms. noise in these maps is 0.97 K, except for the channel at V = 396 km s^{-1} which has a higher noise level due to interference

from the nucleus in PA 27°. The radio power of the nuclear source is given by log P_{21} (W Hz^{-1}) = 18.6. If the other source is also associated with the galaxy, it has log P_{21} = 19.20 and is quite comparable to the young supernova remnant in NGC 4449 (De Bruyn et al. 1981), which has log P_{21} = 19.66 if at 5 Mpc distance.

From VLA observations at 6 cm, Fabbiano et al. (1989) report a tentative nuclear source of S = 0.9 mJy, while Sadler et al. (1989) report an upper limit of 0.8 mJy.

4.2. Channel maps

We subtracted an average of the continuum channel maps from the channel maps which contain both continuum and line emission, in order to properly remove the frequency-dependent grating spikes and sidelobes of the continuum sources. These line channel maps were CLEANed (Högbom 1974; Schwarz 1978), and restored using a Gaussian beam with a HPBW = 34″ × 37″ ($\Delta\alpha \times \Delta\delta$). The resulting maps are shown in Fig. 3.

4.3. Global profile and HI content

We obtained a global 21-cm line profile by integrating the channel maps in an area surrounding the HI emission, and correcting for the attenuation by the primary beam of the VLA telescopes. The resulting global profile is shown in Fig. 4, and its parameters are summarized in Table 3.

Single-dish observations of NGC 5102 have been published by Balkowski et al. (1972), Bottinelli et al. (1970), Bottinelli & Gouguenheim (1976), Gallagher et al. (1975), and Reif et al. (1982). We have compared the VLA global profile with the data from Reif et al. (1982), see Table 3. We find a central velocity of 470±5 km s^{-1}, a profile width at the 50% level of 199±5 km s^{-1}, and a total HI mass of M_{HI} = 0.19 × 10^9 $M_\odot$. This HI mass is 44% less than that derived by Reif et al. (1982), if scaled to the same distance; the latter is some 25% higher than that found by Gallagher et al. (1975), a difference consistent with the observational errors. It is possible that the VLA synthesis observations have missed a significant amount of extended structure. For the systemic velocity and profile width, however, the agreement with Reif et al. is excellent.

The study of Wardle & Knapp (1986) shows that only 7% of all observed lenticulars have a similar, or larger, M_{HI}/L_B-ratio than NGC 5102. Hence, NGC 5102 is quite gas-rich for an S0 galaxy. [Note that the group of galaxies of which NGC 5102 is a member (Sect. 5.3) contains several peculiar, gas-rich galaxies.]

4.4. HI distribution and velocity field

Figure 5 is the map of the HI column density distribution with a resolution of 34″ × 37″ ($\Delta\alpha \times \Delta\delta$), superposed on a blue photograph of the galaxy. In making this map, we used the so-called "conditional-transfer" method (Bosma 1981a). This method serves to suppress the noise and yet to bring out as much faint, extended, structure as possible. In the full-resolution channel maps those pixels were added where in the corresponding

Table 3. Derived global properties for NGC 5102

Assumed distance	4.0 Mpc	*
HI flux	50 Jy km s^{-1}	*
	89.4 Jy km s^{-1}	R
M_{HI}	0.34 × 10^9 $M_\odot$	*
M_{HI}/L_B^0	0.12 $M_\odot/L_\odot$	*
Systemic vel., heliocentric	470 km s^{-1}	*
	471 km s^{-1}	R
HI velocity width		
at 50% level, W_{50}	199 km s^{-1}	*
at 20% level, W_{20}	214 km s^{-1}	*
	215 km s^{-1}	R
M_T (within 6.1 kpc)	1.2 × 10^{10} $M_\odot$	*
M_{HI}/M_T	0.028	*
M_T/L_B^0	4.4 $M_\odot/L_\odot$	*
Continuum flux density, S_{21}	1.9 mJy	*
Radio power: log P_{21}	18.6 (W Hz^{-1})	*

References: R: Reif et al. (1982), *: this paper

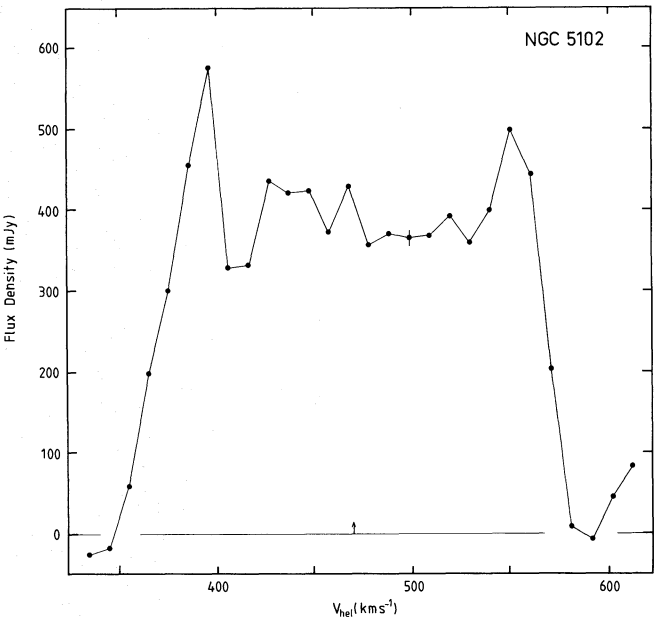

Fig. 4. Global HI profile of NGC 5102, made as explained in the text. The typical rms. uncertainty in the measurements is ±9 mJy

channel maps, smoothed to a 60″ × 60″ beam size, the brightness temperature exceeded 0.88 K (2σ).

The average radial distribution of the HI surface density, σ_{HI} (corrected to face-on), is shown in Fig. 6. This distribution was derived by averaging the full-resolution HI column density map of Fig. 5 (after deprojection) over circular rings in the plane of the galaxy, centered on its nucleus. For the centre position, inclination, and major axis position angle, the values listed in Table 1 were used. In order to avoid confusion, we express face-on surface densities σ_{HI} (projected on the plane of the galaxy) in $M_\odot$ pc^{-2}, and observed column densities N_{HI} (projected on the plane of the sky) in atoms cm^{-2}. The conversion of units is

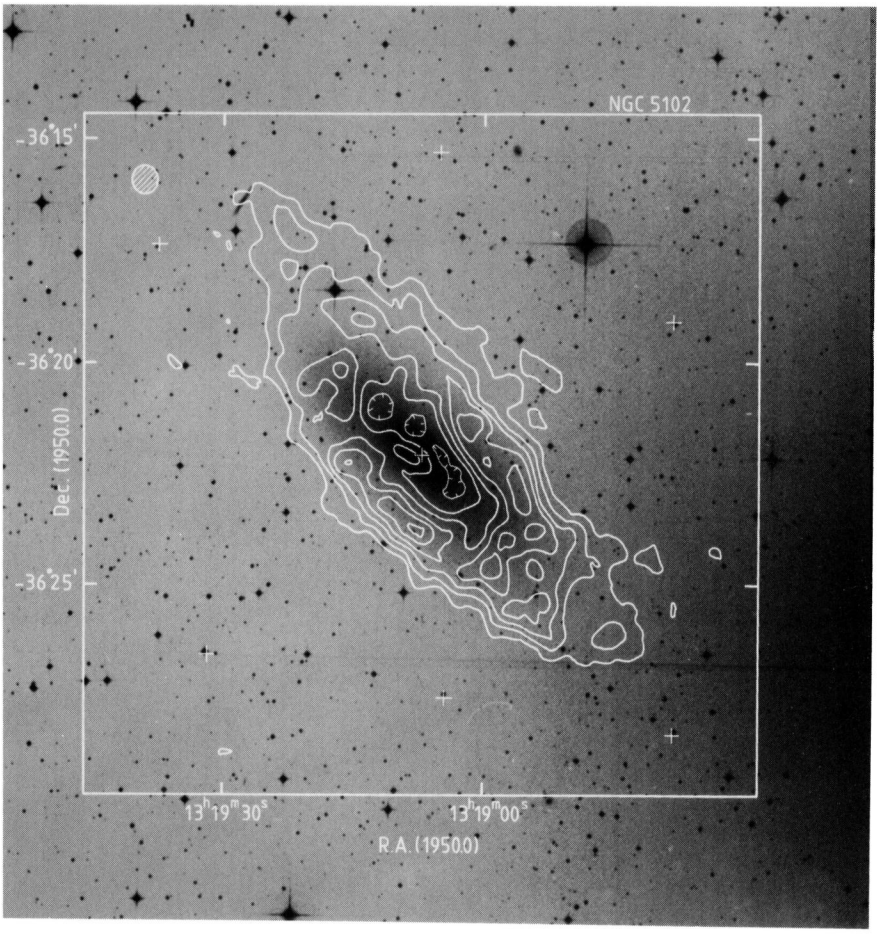

Fig. 5. Contours of the HI column density distribution of NGC 5102 superposed on a blue photograph (cf. Fig. 1). The map was made as explained in the text. Contour values are N_{HI} = 1.4, 2.7, 4.0, 5.4, 6.8, and 8.2 × 10^{20} cm^{-2}. The hatched ellipse shows the beam size $\Delta\alpha \times \Delta\delta = 34'' \times 37''$. The central cross indicates the optical centre, the other crosses are fiducial marks indicating reference star positions

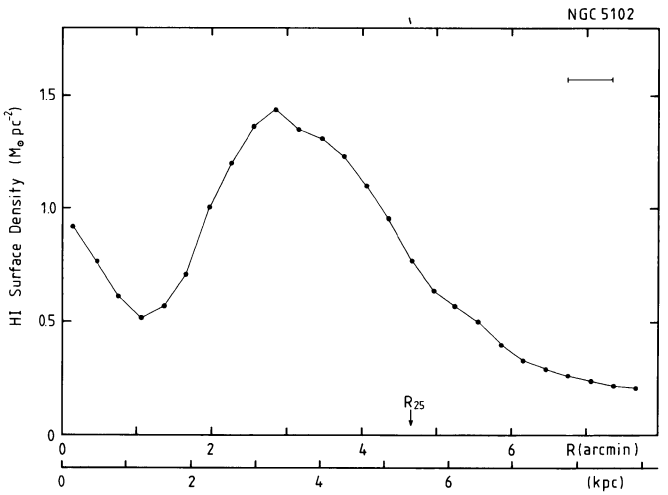

Fig. 6. Radial distribution of the azimuthally averaged HI surface density, σ_{HI} (corrected to face-on), in NGC 5102, derived as explained in the text. The de Vaucouleurs' radius (R_{25}) is shown, as well as the average beam size (top right)

10^{20} atoms cm^{-2} = 0.80 $M_\odot$ pc^{-2}. For a thin flat disk of gas of inclination i to the plane of the sky, $\sigma_{HI} = N_{HI} \cos i$. For NGC 5102, $\cos i$ = 0.34.

Figures 5 and 6 show that the size of the HI distribution in NGC 5102 is not much larger than its de Vaucouleurs' diameters. The HI radius at a level σ_{HI} = 1 $M_\odot$ pc^{-2} is 4.′2 (= 0.91 R_{25}), or 5 kpc (Fig. 6). In Fig. 5 the maximum column densities, $N_{HI} \sim 7.5 \times 10^{20}$ atoms cm^{-2}, occur at radii in the plane of about 3.′5 – 4′ (∼0.8 R_{25}). The maximum ring-averaged surface density, σ_{HI} = 1.4 $M_\odot$ pc^{-2}, is comparable to the low values found by us in other S0 and SB0/a galaxies (see van Driel & van Woerden 1991; van Driel 1987). The two faint HII regions in the disk of NGC 5102, at 1.′1 south-east and 1.′6 south of the centre (see Sect. 2.1), lie in a region of high HI surface density. In fact, the largest HII region coincides with the absolute maximum in the HI column density map ($N_{HI} \sim 8.4 \times 10^{20}$ atoms cm^{-2}).

The HI distribution in NGC 5102 has a pronounced central depression, with a HWHM radius of 1.9 arcmin = 2.2 kpc (i.e. 0.41 R_{25} or 9 times the effective bulge radius), though the average surface density rises again close to the centre, where it reaches σ_{HI}=0.9 $M_\odot$ pc^{-2}. (In fact, Fig. 5 shows that the central depression is less strong on the east side, where a small region of higher densities lies close to the centre.) The "supershell" seen in Hα (Sect. 2.1), which lies mostly north and west of the nucleus, falls within the HI depression. Of course, all the surface and column densities mentioned here are averages over considerable areas, the beam size (FWHM) being 0.7 by 2 kpc in the plane of the galaxy.

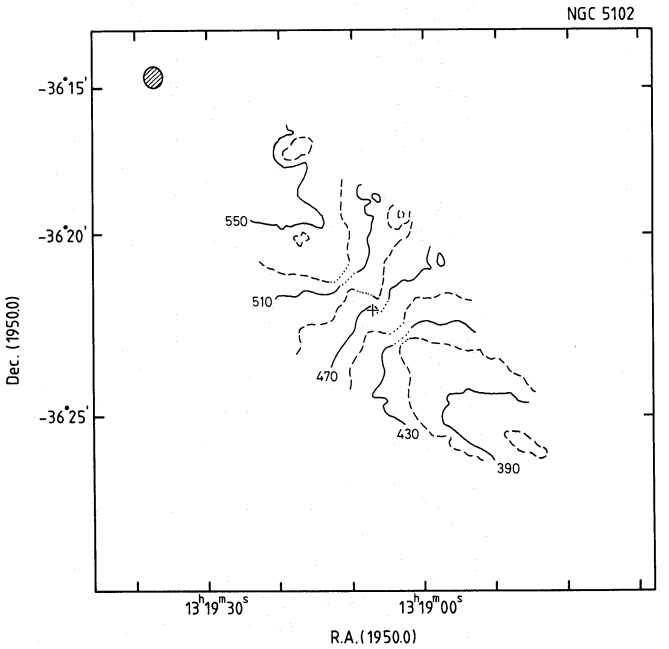

Fig. 7. HI velocity field of NGC 5102 with a resolution (HPBW) of 34″×37″, made as explained in the text. The beam size has been indicated

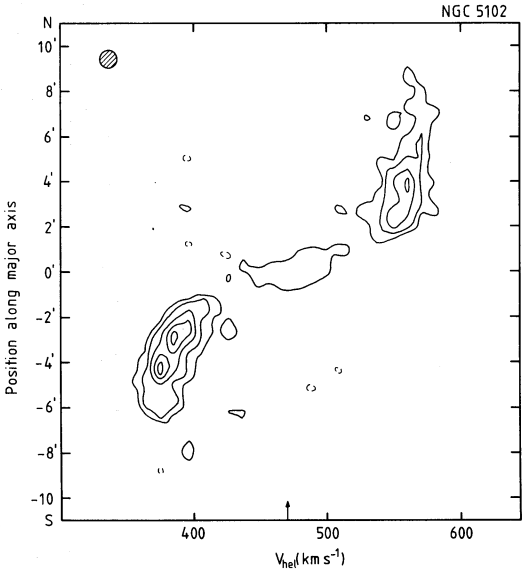

Fig. 8. Position-velocity diagram along the HI kinematical major axis of NGC 5102, a line through the optical nucleus at a position angle of 43°. Contour levels are T_b = −1.6, 1.6, 3.2, 6.5, 9.7, and 12.9 K; negative contours have been dashed. The rms noise in this map is 0.68 K. The FWHM resolution is 12 km s^{-1} × 45″

We made a full-resolution HI velocity field of NGC 5102 by calculating an intensity-weighted mean velocity <V> for each pixel, $<V> = \Sigma[T_b(V)\times V]/\Sigma T_b(V)$. The summation was made over those velocity channels where HI emission was found in the "masked" full-resolution channel maps used in making the integrated HI map (Fig. 5). The resulting velocity field is shown in Fig. 7. The kinematical major axis has an average position angle of 43°, but appears to change somewhat at large radii, especially in the southern part of the disk. Hence, the velocity field of NGC 5102 may show the signature of a slight warp at R > 3′ (see Bosma 1981b). Note that the kinematical minor and major axes are roughly perpendicular. The velocity contours suggest a slight skewing close to the centre, but in view of the low signal-to-noise ratio and the beam size this is not significant.

A position-velocity plot along the kinematical major axis of the HI (Fig. 8) shows the shape characteristic for a galaxy with a flat rotation curve in the outer regions.

4.5. Rotation curve and mass models

Figure 9 is the HI rotation curve, derived from the velocity field on the assumption of circular rotation in a set of concentric (but not necessarily coplanar) rings, centred on the nucleus. The rotation velocities were determined by least-squares fits to the observed velocity field around these rings (Warner et al. 1973; Begeman 1987, 1989). As the velocity field may indicate the presence of a small warp, the position of the centre and the systemic velocity were taken as the only fixed parameters in the model fits, while the inclination and major axis position angle of the rings, together with the rotation velocities, were derived as functions of radius by the least-squares fits. Rotation curves

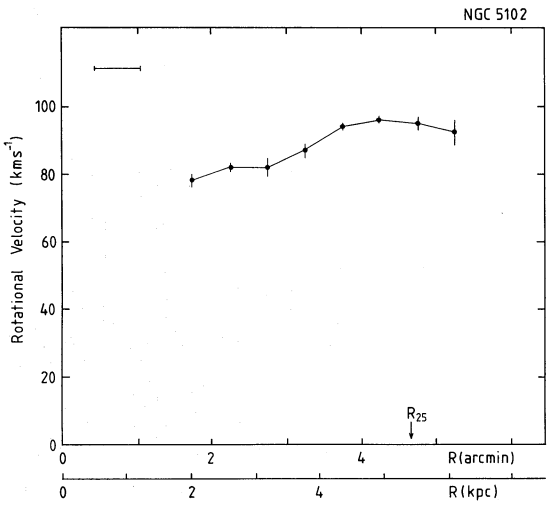

Fig. 9. HI rotation curve for NGC 5102 made by fitting a rotating ring model to the observed velocity field, as explained in the text. The error bars, typically ∼2 km s^{-1}, are standard deviations. The optical de Vaucouleurs' radius (R_{25}) has been indicated, as well as the average beam size

were determined separately for the approaching and receding halves of NGC 5102, and pixels within a sector of ±45° on either side of the minor axis were excluded from the model fits.

Rotation velocities could be measured from R = 2.0 to 6.1 kpc (= 1.1 R_{25}). No significant evidence for a change in inclination with radius was found, though the average major-axis position angles for both halves differ about 6°. Therefore, a rotation curve was then derived using a single inclination (70°) and position angle (43°) for the entire galaxy. The resulting

rotation curve of NGC 5102 is shown in Fig. 9, and summarized in Table 4. The plotted mean errors are of order 2 km s^{-1}. These errors were determined from the fits per ring, and from the difference between the rotation curves of the approaching and receding halves of the galaxy. In the central region no accurate rotation velocities could be measured, not even from the major-axis position-velocity plot, because of beam-smearing effects and the low signal-to-noise ratio.

Table 4. Rotation curve of NGC 5102

Mean HPBW 35″				
Assumed Inclination 70°				
Assumed Major axis p.a. 43°				
Mean radius		V_{rot}	Error	P_{rot}
(arcsec)	(kpc)	(km/s)	(km/s)	(Myr)
105	2.0	78	3	160
135	2.6	82	2	200
165	3.2	82	2.5	240
195	3.8	87	2	270
225	4.4	94	1	290
255	4.9	96	0.5	320
285	5.5	95	2	360
315	6.1	93	3.5	400

The rotation curve is rising in the inner region, but at R > 4 kpc the rotation velocity remains essentially constant at V_{rot} ~95 km s^{-1}. At the outermost radius, R = 6.1 kpc (= 1.1 R_{25}, or 3.5 disk scalelengths), the rotation velocity is 93 km s^{-1}. Using a spherical mass model, this would imply a total mass $M_T = 1.2 \times 10^{10}$ $M_\odot$, or $M_T/L_B^0 = 4.4$ $M_\odot/L_\odot$, within R = 6.1 kpc. At the de Vaucouleurs' radius, R_{25} = 5.4 kpc, the total mass-to-light ratio of NGC 5102 is somewhat smaller than the average value of the S0 and S0/a galaxies in our HI sample, ~7 $M_\odot/L_\odot$ (see van Driel & van Woerden 1991; van Driel 1987).

We have derived a Tully-Fisher relation (see previous two references) between the rotation velocity and blue luminosity for the early-type disk galaxies in our sample, and for a comparison sample of spiral galaxies. NGC 5102 lies close to the mean relation found. Hence, from this relation we find no evidence that NGC 5102 might be 'overluminous' as a result of its recent star formation activity. On the other hand, the agreement of NGC 5102 with the Tully-Fisher relation supports the distance of 4 Mpc assumed by us.

We have attempted to fit a mass model for NGC 5102, consisting of an $r^{1/4}$ bulge, exponential disk and isothermal, spherical dark halo, to the HI rotation curve and optical surface photometry (see e.g. Begeman 1987, 1989; van Albada & Sancisi 1986; van Driel et al. 1988a). Satisfactory fits are obtained for a wide range of values of the halo core radius and halo mass, as well as the disk and bulge masses, even if the scale length of the disk, the effective radius of the bulge, and the disk-to-bulge mass ratio are kept constant. The present rotation data do not provide adequate constraints to the three-component mass models; for this, an optical rotation curve would be required in addition.

A mass model consisting of only a disk component with the adopted scalelength of 1.8 kpc (see Sect. 2.1 and Table 1) would be unsatisfactory, and a bulge + disk model without a halo (cf. that for M31 by Braun 1991) would give a poor fit to the data. However, the failure of these simpler solutions could in principle be removed by allowing a mild warp of order 20°, or large-scale noncircular motions of order 10 km s^{-1}. Since neither of these distortions can be clearly excluded, the present data do not prove that a dark halo is present in NGC 5102.

5. Discussion

With a distance of 4 Mpc NGC 5102 is one of the nearest gas-rich S0 galaxies, in fact the nearest in the sample discussed in the present series of papers (cf. van Driel and van Woerden 1991, Paper XI). Consequently the linear resolution of our HI observations, 700 pc, is much better than that achieved in other S0 and S0/a galaxies, 1.5 to 3 kpc, and in NGC 5102 we can observe detail inaccessible elsewhere. On the other hand, NGC 5102 is one of the smaller galaxies in our sample, with D_{25} = 11 kpc and $M_B = -18.1$, and the relative resolution obtained, 0.064 D_{25}, is only slightly better than that in some other galaxies. The small distance has the further advantage of making lower levels of star formation observable.

We shall now compare the observed HI properties of NGC 5102 to those of other gas-rich S0 galaxies and of early-type spirals, and discuss the possible significance of these findings to the evolution of the system.

5.1. Summary of HI properties, and comparison to other S0 galaxies

The HI distribution (Figs. 5 and 6) lies mostly within the optical boundaries. The radial distribution of (azimuthally averaged) surface density, σ_{HI}, peaks at R = 0.6 R_{25}, with σ_{HI} = 1.4 $M_\odot/pc^2$, and falls to half that value at R = 0.35 and 1.03 R_{25}. The average value of σ_{HI} is similar to that in other gas-rich lenticulars. However, while the majority of gas-rich lenticular galaxies in our sample have most of their HI in the outer parts, or indeed outside the optical boundaries, the HI distribution in NGC 5102 is dominated by this inner ring of R ~ 0.7 R_{25}. Inner HI rings of radius $R_r \sim 0.4\,R_{25}$ were found in NGC 2685 (Shane 1980), NGC 3900 (Paper VIII), 3941 (Paper IX), 4203 (Paper V), 5101 (Paper VII), and 7013 (Paper II), but all these inner rings contain only a minor fraction of the gas in the galaxy, and in all cases but one (NGC 3900) they occur in combination with an outer HI ring. The only other galaxy in our sample where most of the HI lies in an "inner ring" is NGC 3998 (Paper III), with $R_r \sim 0.7\,R_{25}$; but this is a *polar* ring. Hence, NGC 5102 is the only galaxy in our sample with the HI concentrated in an inner ring aligned with the stellar disk.

The rotation speed in this HI ring rises slightly outward from ~80 km/s at 0.4 R_{25} to ~95 km/s at 0.8–1.1 R_{25}. The values of rotation speed and luminosity fit the Tully-Fisher relation,

indicating that dynamically NGC 5102 is similar to other disk galaxies.

Within the HI ring several condensations of a few kpc size are observed, a situation similar to that in other galaxies in our sample. The brightest condensation, 1.7 arcmin S of the centre, has a peak column density $N_{HI} = 8 \times 10^{20}$ atoms/cm^2 (as observed at 700 pc resolution!), and is associated with a faint HII region observed by van den Bergh (1976). This result appears consistent with the threshold for star formation, $\sigma_{HI} \sim 1 \times 10^{21}$ cm^{-2}, found by Skillman (1987) in irregular galaxies at ~500 pc resolution.

Within the central depression of radius 0.35 R_{25}, we find in NGC 5102 a secondary maximum of $\sigma_{HI} = 0.9$ $M_\odot$/pc^2 at the centre of the galaxy. (In fact, this maximum lies on a tongue reaching into the centre from the east.) We have not found such a central maximum in other S0 galaxies, but this may be due to lack of linear resolution.

The blue integrated colour, $(B-V)_T^0 = 0.58$, and early-type (A–F) spectrum make NGC 5102, together with the peculiar S0 galaxy NGC 4694 (Van Driel & Van Woerden 1989), exceptional within our sample. (Only the extreme dwarf UGC 12713, with $M_B = -14.0$, is bluer.) These properties – and, in fact, several others – are very similar to those of spiral galaxies.

5.2. Comparison with spiral galaxies

The integrated colour of NGC 5102 is normal for spiral galaxies of type Sbc (de Vaucouleurs 1974). However, the colour gradient (bluer towards the centre) is unusual, and so is the bright and quite blue nucleus ($M_B = -14$, $(B-V)_0 = +0.2$) observed by Pritchet (1979).

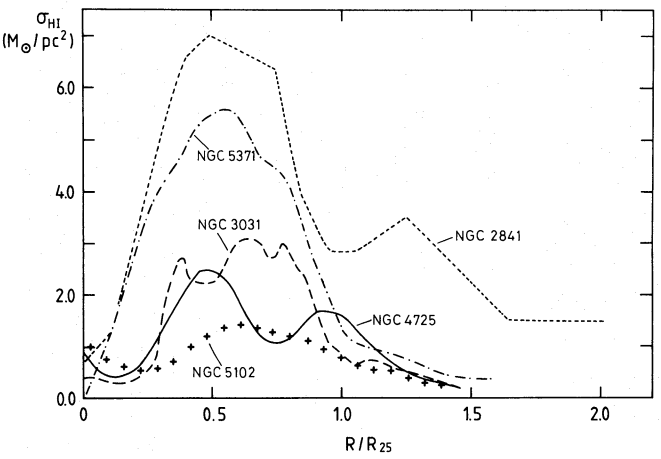

Fig. 10. Azimuthally averaged HI surface densities in NGC 5102 and a number of early-type spirals. The surface densities are plotted as functions of radius, relative to R_{25}

The overall gas content of NGC 5102 may be characterized by the distance-independent ratio between HI mass and blue luminosity, $M_{HI}/L_B = 0.12$. We compare this value with the (logarithmic) averages per morphological type, found by Shostak (1978): 0.21 for Sbc, by Bottinelli et al. (1980): 0.15 for S0/a-Sab, and by Huchtmeier (1982): 0.10 for Sa. The value 0.12 for NGC 5102 appears normal for type Sa or Sab – with considerable latitude, since the dispersions per type are a factor ~2 in M_{HI}/L_B.

In Figure 10 we compare the radial distributions of HI surface density σ_{HI} (azimuthally averaged) in NGC 5102 and in several early-type spirals. The radial coordinate has been scaled to the "de Vaucouleurs radius" $R_{25} \equiv \frac{1}{2}D_{25}$. The HI distribution in M81 = NGC 3031 (type Sb(r)I–II, Sandage & Tammann 1981) shows a plateau of $\sigma_{HI} \sim 2.7$ $M_\odot$/pc^2 between $R/R_{25} = 0.35$ and 0.85 (Rots & Shane 1975). In NGC 4725 (type Sb/SBb(r)II) σ_{HI} reaches a peak of 2.5 $M_\odot$/pc^2 at 0.5 R_{25}, with a secondary maximum at 0.95 R_{25} (Wevers et al. 1984, 1986). The Sb-type galaxy NGC 2841 (Begeman 1987) and Sb/SBb-type NGC 5371 (Wevers et al. 1986) have maxima of 7 and 5.5 $M_\odot$/pc^2 around $R/R_{25} = 0.5$–0.6, with half-maximum values at $R/R_{25} = 0.2$ and 0.9 in both. Although the surface densities in NGC 5102 are lower, the shape and location of its HI distribution are fairly similar to those in the four Sb spirals. (However, in the spirals with greater HI surface densities the edges of the distribution appear to be steeper.) Note that NGC 4694, whose colour is very similar to that of NGC 5102, has a very different HI distribution: a small central condensation and an extended tail of ~40 kpc length, i.e. > 5 R_{25} (Van Driel & Van Woerden 1989).

The HI in NGC 5102 shows no spiral structure, and its small-scale structure is less developed than in NGC 3031 (SbI-II) and 2841 (Sb), but it appears similar to that in NGC 5371 (Sb/SBbI) and in NGC 4242 (SBdIII, Wevers et al. 1986), the latter having similar luminosity to NGC 5102.

A major difference between NGC 5102 and spiral galaxies is in the strength and distribution of star formation. In spiral galaxies, young stars (age < 10^8 yrs) are concentrated in the spiral arms, and stars of types A and F are widely distributed throughout the disk. In NGC 5102, van den Bergh (1976) and Danks et al. (1979) have found some evidence for recent star formation sprinkled over the disk (but not in spiral arms); the distributions of colour and spectrum (Sect. 2.1) indicate that (2–3) × 10^7 $M_\odot$ of stars have formed a few times 10^8 yr ago within ~1 kpc from the centre, with a strong peak at the centre.

5.3. The environment of NGC 5102

In view of the possible influence of the environment on the evolution of a galaxy, we have searched for galaxies which may lie within 1 Mpc of NGC 5102. Table 5 lists objects found from the RC2, the EUS (Lauberts 1982), from Fisher and Tully (1981), or from Huchtmeier and Richter (1989), and satisfying the following criteria: 1) position within 15° of NGC 5102, and 2) radial velocity within 200 km/s of that of NGC 5102 (471 km/s). The second criterion was chosen to allow for an appropriate velocity dispersion within a group of galaxies. We note the following facts.

Table 5 contains 12 objects which may lie within 1 Mpc of NGC 5102. These objects, plotted in Fig. 11, all probably

Table 5. Environment of NGC 5102: probable members of NGC 5128 group

Name	EUS nr.	α(1950)	δ(1950)	Type	D×d arcmin	B_T mag	Ref	Θ	V_{hel} (km/s)	Ref
	381G20	$12^h43^m18^s$	−33°33′9	Irr	4.5:×1.8:	14.1±0.3	a	7°6	585±5	a
NGC 4945	219G24	13 02 31	−49 12.2	Sc-Irr	26.0:×6.0:	9.60±0.13	b	13.2	563±14	b
NGC 5102	382G50	13 19 07	−36 22.2	SO	12.0:×5.0:	10.35±0.12	c	0.0	471±8	d
NGC 5128 =Cen A	270IG9	13 22 33	−42 45.4	(EO+Sb)?	30.0:×23.0:	7.96±0.10	c	6.4	526±8	b
	324G24	13 24 42	−41 13.3	Dwarf Irr	4.5:×3.4:	13.9±0.3	a	4.9	512±5	a
Fourcade-Figueroa	270G17	13 31 39	−45 17.1	S.../Irr	17.0:×2.0:	12.1±0.8	a	9.3	825±5	a
									828±4	d
	444G78	13 33 42	−28 58.9	Dwarf	1.7:×0.7:			8.0	570±2	e
NGC 5236 =M83	444G81	13 34 11	−29 36.8	Sc	18.0:×18.0:	8.51	b	7.4	520±6	b
	444G84	13 34 32	−27 47.5	Dwarf	1.6:×1.3:	15.0±0.8	a	9.0	590±5	a
NGC 5237	270IG22	13 34 40	−42 35.6	SO	1.9:×1.6:	13.39	f	7.2	373±22	f
NGC 5253	445G4	13 37 05	−31 23.5	E-SO	6.0:×2.0:	10.99±0.09	c	6.1	410±6	d
IC 4316	445G6	13 37 29	−28 38.5	Irr	1.6:×1.3:	16.41	h	8.5	719±90	g
NGC 5264	445G12	13 38 47	− 29 39.7	S.../Irr?	3.5:×3.0:	12.64±0.05	j	7.7	478±10	a
	325G?11	13 42 01	−41 36.5	Dwarf Irr.?	4.0:×2.0:	14.1±0.8	a	6.9	540±5	a
	383G87	13 46 23	−35 48.8	Dwarf spiral	6.0:×5.5:	11.3 ±0.8	a	5.5	330±4	a
NGC 5408	325G?47	14 00 18	−41 08.2	Irr?	2.6:×1.6:			8.0	510±8	k

References: a: Webster et al. 1979, b: Sandage & Tammann 1981 (RSA), c: De Vaucouleurs et al. 1976 (RC2), d: Reif et al. 1982, e: Huchtmeier & Richter 1986, f: West et al. 1981, g: Penston et al. 1977, h: Bohuski et al. 1978, j: De Vaucouleurs et al. 1981, k: Fisher & Tully 1981

belong to De Vaucouleurs' (1975) group G4. The group appears to contain two subgroups, and is known to include a number of peculiar galaxies. The northern subgroup, centred on NGC 5236, a spiral of very high surface brightness, contains within a projected radius of only 120 kpc four dwarf-irregular objects of absolute magnitude −12 to −15, and the peculiar (IO?) galaxy NGC 5253 of $-17^m.6$. The southern subgroup, centred on NGC 5128 (the radio galaxy Centaurus A), contains within 300 kpc radius two dwarf irregulars and a dwarf-S0 galaxy; the large irregular EUS 270–G17 (the Fourcade-Figueroa object) may or may not belong to the group. NGC 4945 lies fairly isolated, NGC 5068 (at 15°.6 North) belongs to a separate (sub)group. The nearest neighbours of NGC 5102 are at projected distances of order 400 kpc; NGC 5128 and NGC 5236, the two dominating members of the group, are at 6°.4 = 450 kpc and 7°.4 = 520 kpc, respectively.

As noted by Webster et al. (1979), whose results have been incorporated into Table 5 and Fig. 11, the group G4 contains many low-surface-brightness (dwarf) galaxies. While their observations do not represent any complete sample, there is no reason to assume that the concentrations around NGC 5128 and NGC 5236 are caused by observational selection.

The dispersion σ_V of the 13 radial velocities measured from the 21-cm line is 73 km/sec, in keeping with the 1 Mpc radius of the group. If the group is in virial equilibrium, its total mass should be of order $M \sim 6\ R(\sigma_V)^2/G \sim 7 \times 10^{12}\ M_\odot$. Since, with the B_T-values from Table 5, and distance 4 Mpc, the total blue luminosity is $L_B = 3.4 \times 10^{10}\ L_\odot$, we find a mass/luminosity ratio of order 200 for the group. With mutual velocities of order 100 km/sec, any encounter of NGC 5102 with another galaxy in the search area would have occurred at least $\sim 4 \times 10^9$ yr ago.

5.4. A possible evolutionary scenario for NGC 5102

Gas-rich S0 galaxies are fairly rare. But among gas-rich S0's, NGC 5102 is unique in several respects: 1) its HI distribution resembles that of spiral galaxies, rather than of other S0's; 2) its colour is blue, like that of spirals; 3) major star formation has recently (<1 Gyr ago) occurred in the innermost regions of this galaxy. The major questions to be answered are, in other words: a) Why is this gas-rich galaxy not a spiral? b) Why is it nevertheless blue? c) Why has it undergone star formation in its nucleus?

While the gas/blue-light ratio and the radial HI distribution in NGC 5102 are similar to (and the average surface density of HI slightly lower than) those in early-type spirals, the HI distribution shows no spiral pattern. Spirality is generally stronger in the more luminous spirals, but it is also seen in stars and gas in objects like M33 (Deul & Van der Hulst 1987), which have luminosities similar to NGC 5102 (but later morphological types). In this connection, it may be significant that NGC 5102 has no near neighbours: as shown in the previous section, no major encounter with another galaxy is likely to have occurred in the last 4×10^9 yr. Therefore, the swing amplifier mechanism proposed

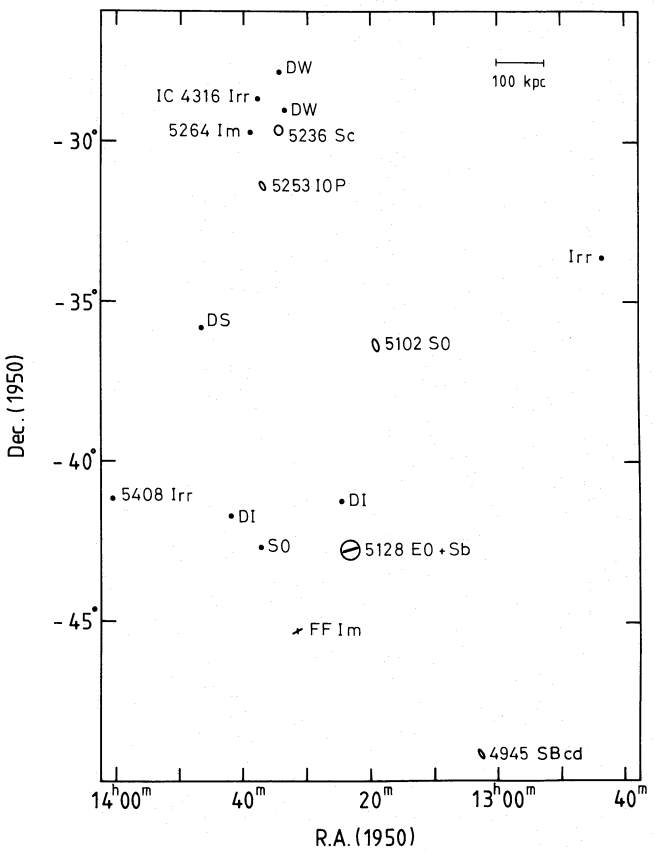

Fig. 11. Environment of NGC 5102. Only galaxies which may belong to the same group are plotted. Optical sizes are plotted to scale, NGC and IC numbers are given, and morphological type codes shown (DI = dwarf irregular, DS = dwarf spiral, DW = dwarf, Im = magellanic irregular, Irr = irregular, IOP = peculiar amorphous irregular). FF= Fourcade-Figueroa object

by Toomre (1981), which successfully explains spiral structure in small groups of galaxies in terms of close encounters, would not recently have had a chance in NGC 5102, and this galaxy may not have had any spiral structure since half a Hubble time. For lack of a suitable driver, then, major star formation may have been virtually absent in NGC 5102 since several Gyr, except in the nucleus. Though substantial amounts of gas were available, local densities may have remained generally too low for effective star formation.

However, it would be incorrect to consider the disk of NGC 5102 "burnt out", i.e. to have consumed its gas in star formation, in the sense of Larson et al. (1980). Given a suitable trigger, extensive star formation would be possible in this gas-rich galaxy. The majority of S0 galaxies have far smaller amounts of gas than NGC 5102.

Alternatively, NGC 5102 may have "burnt out" virtually completely several Gyr ago, like other S0's, and then acquired its present gas supply by (fairly recent) capture of a gas-rich dwarf galaxy. With $M_{HI} \sim 3 \times 10^8$ $M_\odot$ and an M_{HI}/L_B ratio of 1, this dwarf would have had absolute magnitude -16 and a mass probably of order 10^9 $M_\odot$, i.e. a few percent of that of NGC 5102. Given the regular distribution and rotation of the gas, and the very smooth light distribution in the galaxy, we must assume that a few rotation periods have passed since the event. The rotaton period is 270 Myr at R = 0.7 R_{25}. Hence, the hypothetical capture would have occurred at least ~800 Myr ago.

Unlike in spiral galaxies, the blue colour of NGC 5102 is not due to recent star formation within the main body of a gas-rich disk. Strong star formation has occurred recently only at distances less than 1 kpc from the centre. From UBVR photometry, Pritchet (1979) estimates that 2×10^7 $M_\odot$ of stars have been formed in the last 10^8 yr; and Glass & Moorwood (1984), from infrared colours, suggest that a starburst occurred about 5×10^8 yr ago. The central depression in the HI distribution (Fig. 6) is of interest in this connection. From an originally flat surface density distribution with σ_{HI} = 1.5 $M_\odot/pc^2$ between R = 0 and 0.6 R_{25} = 3 kpc, a total of 1.5×10^7 $M_\odot$ of HI would have to be removed to make the present hole. Adding 0.5×10^7 $M_\odot$ of helium, this amount of gas would be consistent with that required by Pritchet for recent star formation. However, the radial distribution of the young stellar component is much more strongly peaked at the centre than the HI depression, and any relationship between these two distributions remains hypothetical. Little is known yet about the possible presence and radial distribution of molecular gas in NGC 5102. [A recent observation by Tacconi et al. (1991) with SEST at La Silla indicates an upper limit of order 2×10^7 $M_\odot$ to the mass of molecular hydrogen within ~2 kpc radius. This limit is still compatible with the amount of HI "missing" in the central depression.] Detailed CO observations would clearly be of great interest.

Even if the distribution of young stars is related to the central HI depression, the cause of the "starburst" remains unclear. Have the inner parts of the gas distribution collapsed into the centre? A detailed analysis of the distribution of stellar ages in the central kpc might shed light on this issue, but this represents a difficult observational problem.

Alternatively, the "starburst" may possibly have been caused by infall of $\sim 10^7$ $M_\odot$ of gas from outside into the nucleus of the galaxy. Such an amount represents the gas content of a small dwarf galaxy of absolute magnitude -14, or apparent magnitude +14. Objects of this sort are abundant in the surroundings of NGC 5236 and 5128. Although they have not been found close to NGC 5102, the inventory given in Table 5 and Fig. 11 is probably incomplete, since for the majority of the objects listed in the ESO-Uppsala Catalogue no redshift is known.

With a rotation period of order 100 Myr at 1 kpc from the centre, the distribution and motions of gas in the innermost kpc might well show vestiges of the recent starburst and of its cause, whether radial collapse of the gas disk or infall of a dwarf galaxy. More detailed and sensitive observations of HI and CO would be required for this purpose. The tongue of HI seen east of the nucleus in Fig. 5, though in need of confirmation, may be significant in this connection – as may the "supershell" of Hα reported by Ciardullo et al. (1988).

5.5. NGC 5102: an amorphous irregular galaxy?

In some respects, NGC 5102 appears to be similar to the class of amorphous irregulars described by Sandage & Brucato (1979). These objects are characterized by smooth optical appearance, but — in contrast to elliptical galaxies — blue colours and intense emission lines. In terms of global properties, such as surface brightness, mass, luminosity, rotation, metallicity, gas fraction and star formation rate, the amorphous irregulars resemble the magellanic irregulars (Hunter & Gallagher 1986; Gallagher et al. 1981). However, amorphous irregulars have a dominant central supergiant star-forming complex rather than an irregular distribution of young stars.

NGC 5102 indeed is optically smooth and blue. Its mass, luminosity and rotation speed are similar to those of the Large Magellanic Cloud; gas fraction and star formation rate are lower. The intense emission lines typical of the class of amorphous irregulars are lacking. A central supergiant star-forming complex may not be present now, but must have existed some 10^8 years ago. Hence, NGC 5102 may be viewed as an "aging amorphous irregular galaxy".

A more complete comparison would profit from availability of detailed HI maps of amorphous irregulars. Such maps are at present in preparation by Hunter, van Woerden and Gallagher.

6. Conclusions and possible follow-up

NGC 5102 is a low-luminosity disk galaxy of absolute magnitude -18 and with the smooth optical morphology typical of a pure S0 galaxy. The HI extent and radial distribution are similar to those in early-type spirals, but neither gas nor stars show any spiral pattern. Current star formation in the disk is sparse, but there has been a strong starburst 10^{8+} years ago in the nuclear region.

The HI disk may be old, partly burnt-out and "smouldering", or it may have been acquired by fairly recent capture ($\gtrsim$1 Gyr ago) of a gas-rich, smaller galaxy (-16^{M}). The nuclear starburst could be due to radial collapse of the inner parts of the gas distribution, or to recent infall of a gas-rich dwarf of -14^{M}.

Our understanding of this galaxy would be fostered by various new observations. Detailed spectroscopy would be required to measure the chemical composition and stellar age distribution in the nuclear region. An optical rotation curve for the inner parts of the galaxy would be useful. A CO map may show whether molecular gas has played a role in the central starburst. Further analysis of the structure and kinematics of the Hα supershell (Sect. 2.1) should reveal details of these effects. Also, a more detailed and sensitive study of HI distribution and motions in the nuclear region may reveal effects — and possibly even the cause — of the starburst. A thorough comparison to the class of amorphous irregulars would also be of interest.

Acknowledgements. We wish to thank Drs. E.A. Valentijn and A. Lauberts for the use of their surface photometry in advance of publication, L.G. Sijbring for his help in fitting the luminosity profile, Dr. A.C. Danks for the use of his CCD images, Dr. K. Begeman for his help in the mass model fitting, and Drs. R. Ciardullo and G.H. Jacoby for making their observations of Hα and [O III] available to us. We further thank Dr. D. Burstein and especially Dr. G.H. Jacoby for their comments. We have made use of the NASA/IPAC Extragalactic Database (NED) which is operated by the Jet Propulsion Laboratory, California Institute of Technology, under contract with the U.S. National Aeronautics and Space Administration. W.v.D. has been supported by the Netherlands Organization for the Advancement of Pure Research (ZWO) through the ASTRON foundation, H.v.W. by NATO through research grant RG 98.82.

References

Allen, R.J., Ekers, R.D., Terlouw, J.P. 1985, in Proc. Intern. Workshop on Data Analysis in Astronomy at Erice, ed. V. di Gesu, Plenum, London, p. 271
Alloin, D., Bica, E. 1989, A&A, 217, 57
Balkowski, C., Bottinelli, L., Gouguenheim, L., Heidmann, J. 1972, A&A, 21, 303
Balkowski, C., Alloin, D., Le Denmat, G.: 1986, A&A, 167, 223
Begeman, K. 1987, HI Rotation Curves of Spiral Galaxies, Ph.D. thesis, Groningen University, The Netherlands
Begeman, K. 1989, A&A, 223, 47
Bica, E. 1988, A&A, 195, 76
Bica, E., Alloin, D. 1987a, A&AS, 70, 281
Bica, E., Alloin, D. 1987b, A&A, 181, 270
Bica, E., Alloin, D. 1987c, A&A, 186, 49
Bohuski, T.J., Fairall, A.F., Weedman, D.W. 1978, ApJ, 221, 776
Bosma, A. 1981a, AJ, 86, 1791
Bosma, A. 1981b, AJ, 86, 1825
Bonatto, C., Bica, E., Alloin, D. 1989, A&A, 226, 23
Bottinelli, L., Chamaraux, P., Gouguenheim, L., Lauqué, R. 1970, A&A, 6, 453
Bottinelli, L., Gouguenheim, L. 1976, A&A, 47, 381
Bottinelli, L., Gouguenheim, L., Paturel, G. 1980, A&A, 88, 32
Braun, R. 1991, ApJ, 372, 54
Burstein, D. 1979, ApJ, 234, 435
Burstein, D., Davies, R.L., Dressler, A., Faber, S.M., Stone, R.P.S., Lynden-Bell, D., Terlevich, R.J., Wegner, G. 1987, ApJS, 64, 601
Burstein, D., Bertola, F., Buson, C.M., Faber, S.M., Lauer, T.R. 1988, ApJ, 328, 440
Canizares, C.R., Fabbiano, G., Trinchieri, G. 1987, ApJ, 312, 503
Ciardullo, R., Jacoby, G.H., Ford, H.C. 1988, BAAS, 20, 1081
Danks, A.C., Laustsen, S., van Woerden, H. 1979, A&A, 73, 247
Davies, R.L., Burstein, D., Dressler, A., Faber, S.M., Lynden-Bell, D., Terlevich, R.J., Wegner, G. 1987, ApJS, 64, 581
de Bruyn, A.G., Goss, W.M., van Woerden, H. 1981, A&A, 94, L25
de Jong, T. Clegg, P.E., Soifer, B.T., Rowan-Robinson, M., Habing, H.J. Houck, J.R., Aumann, H.H., Raimond, E. 1984, ApJ, 278, L67
de Jong, T., Brink, K. 1987, in Star Formation In Galaxies, ed. C.J. Lonsdale Persson, NASA Conference Publication 2466, p. 323
Deul, E., and Van der Hulst, J.M. 1987, A&AS, 67, 509
de Vaucouleurs, A., de Vaucouleurs, G. 1967, AJ, 72, 730
de Vaucouleurs, G. 1974, in IAU Symp. 58 The Formation and Dynamics of Galaxies, ed. J.R. Shakeshaft, Reidel, Dordrecht, p. 1
de Vaucouleurs, G. 1975, in Galaxies and the Universe, eds. A.R. Sandage, M. Sandage and J.R. Kristian, Univ. Chicago Press, p. 557
de Vaucouleurs, G., de Vaucouleurs, A., Corwin, H. 1976, Second Reference Catalogue of Bright Galaxies, Univ. of Texas Press (RC2)
de Vaucouleurs, G., de Vaucouleurs, A., Buta, R. 1981, AJ, 86, 1429
de Vaucouleurs, G., Olson, D.W. 1984, ApJS, 56, 91

Dressler, A., Sandage, A. 1983, ApJ, 265, 664
Eggen, O.J. 1971, QJRAS, 12, 306
Evans, D.S. 1952, MNRAS, 112, 606
Evans, D.S. 1963, M.N.A.S.S.A., 22, 140
Fabbiano, G., Gioia, I.M., Trinchieri, G. 1989, ApJ, 347, 127
Faber, S.M., Jackson, R.E. 1976, ApJ, 204, 668
Fisher, J., Tully, R.B. 1981, ApJS, 47, 139
Forman, W., Jones, C., Tucker, W. 1985, ApJ, 293, 102
Gallagher, J.S., Faber, S.M., Balick, B. 1975, ApJ, 202, 7
Gallagher, J.S., Hunter, D.A., Knapp, G.R. 1981, AJ, 86, 344
Gillett F.C., de Jong, T., Neugebauer, G., Rice, W., Emerson, J.P. 1988, AJ, 96, 116
Glass, I.S., Moorwood, A.F.M. 1984, Observatory, 104, 231
Helou, G., Khan, I.R., Malek, L., Boehmer, L. 1989, ApJS, 68, 151
Hjellming, R.M. (editor) 1983, An Introduction to the NRAO Very Large Array, National Radio Astron. Obs., U.S.A.
Högbom, J.A. 1974, A&AS, 15, 417
Huchtmeier, W.K. 1982, A&A, 110, 121
Huchtmeier, W.K., Richter, O.G. 1986, A&AS, 63, 323
Huchtmeier, W.K., Richter, O.G. 1989, General Catalog of HI Observations of Galaxies, Springer, Berlin/New York
Hunter, D.A., Gallagher, J.S. 1986, Publ. Astr. Soc. Pacific, 98, 5
Jacoby, G.H., Ciardullo, R., Ford, H.C. 1988, in The Extragalactic Distance Scale, ed. S. van den Bergh & C.J. Pritchet, ASP Conference Series No. 4 (Provo: Brigham Young University Press), p. 42
Knapp, G.R., van Driel, W., Schwarz, U.J., van Woerden H., Gallagher, J.S. 1984, A&A, 133, 127 (paper II)
Knapp, G.R., van Driel, W., van Woerden, H. 1985, A&A, 142, 1 (paper III)
Knapp, G.R., Guhathakurta, P., Kim, D-W., Jura, M. 1989, ApJS, 70, 329
Krumm, N., van Driel, W., van Woerden, H. 1985, A&A, 144, 202 (paper IV)
Larson, R.B., Tinsley, B.M., Caldwell, C.N. 1980, ApJ, 237, 692
Lauberts, A. 1982, The ESO/Uppsala Survey of the ESO(B) Atlas, European Southern Observatory.
Lauberts, A., Valentijn, E.A. 1985, in New Aspects of Galaxy Photometry, Proc. of the specialized meeting of the eigth IAU European Regional Astronomy Meeting, ed. J.L. Nieto, p. 73
Lauberts, A., Valentijn, E.A. 1989, The Surface Photometry Catalogue of the ESO-Uppsala Galaxies, European Southern Observatory
Lonsdale, C.J., Helou, G., Good, J.C. Rice, W. 1985, Cataloged Galaxies and Quasars Observed in the IRAS Survey, Jet Propulsion Laboratory
Lonsdale, C.J., Helou, G., Good, J.C. Rice, W. 1989, Cataloged Galaxies and Quasars Observed in the IRAS Survey, 2nd version, Jet Propulsion Laboratory
Miller, G.E., Wu, C.C. 1984, BAAS, 16, 949
Moorwood, A.F.M., Oliva, E. 1988, A&A, 203, 278
Penston, M.V., Fosbury, R.A.E., Ward, M.J., Wilson, A.S. 1977, MNRAS, 180, 19
Persson, S.E., Frogel, J.A., Aaronson, M. 1979, ApJS, 39, 61
Pritchet, C. 1979, ApJ, 231, 354
Reif, K., Mebold, U., Goss, W.M., van Woerden, H., Siegman, B. 1982, A&AS, 50, 451
Rice, W., Lonsdale, C.J., Soifer, B.T., Neugebauer, G., Kopan, E.L., Lloyd, L.A., de Jong, T., Habing, H.J. 1988, ApJS, 68, 91
Roberts, M.S., Hogg, D.E., Bregman, J.N., Forman, W.R., Jones, C. 1991, ApJS 75, 751
Rocca-Volmerange, M., Balkowski, C. 1984, in Proc. 4th Europ. IUE Conference, p. 69
Rocca-Volmerange, M., Guiderdoni, B. 1987, A&A, 175, 15
Rots, A.H., Shane, W.W. 1975, A&A, 45, 25
Rots, A.H. 1982, in Synthesis Mapping, NRAO Workshop Proceedings No. 5, ed. A.R. Thompson and L.R. d'Addario, National Radio Astron. Obs.
Sadler, E.M., Jenkins, C.R., Kotanyi, C.G. 1989, ApJ, 240, 591
Sandage, A., Brucato, R. 1979, AJ, 84, 472
Sandage, A., Tammann, G. 1981, A Revised Shapley-Ames Catalog of Bright Galaxies, Carnegie Institute of Washington (RSA)
Schwarz, U.J. 1978, A&A, 65, 345
Sérsic, J.L. 1968, Atlas de Galaxias Australes, Cordoba Univ. Obs., Argentina
Shane, W.W. 1980, A&A, 82, 314
Shostak, G.S. 1978, A&A, 68, 321
Simien, F., de Vaucouleurs, G. 1986, ApJ, 302, 564
Skillman, E.D. 1987, in Star Formation in Galaxies, ed. C.J. Lonsdale Persson, NASA Conference Publication 2466, p. 263
Spitzer, L. 1978, Physical Processes in the Interstellar Medium, Wiley and Sons, New York
Tacconi, L.J., Tacconi-Garman, L.E., Thornley, M., van Woerden, H. 1991, A&A, 252, 541
Toomre, A. 1981, in The Structure and Evolution of Normal Galaxies, eds. S.M. Fall & D. Lynden Bell, Cambridge Univ. Press, p. 111
Trinchieri, G., Fabbiano, G. 1985, ApJ, 296, 447
van Albada, T.S., Sancisi, R. 1986, in Material Content of the Universe, Phil. Trans. Roy. Soc. London A320, 447
van den Bergh, S. 1976, AJ, 81, 795
van den Broek, A.C. 1990, A Study of Extreme IRAS Galaxies, Ph.D. Thesis, University of Amsterdam, The Netherlands
van den Broek, A.C. 1992, in preparation
van Driel, W. 1987, A Study of HI in S0 Galaxies, Ph.D. thesis, Groningen University, The Netherlands, chapter 3
van Driel, W., van Woerden, H., Gallagher, J.S., Schwarz, U.J. 1988a, A&A, 191, 201 (paper V)
van Driel, W., Davies, R.D., Appleton, P.N. 1988b, A&A, 199, 41 (paper VI)
van Driel, W., Rots, A.H., van Woerden, H. 1988c, A&A, 204, 39 (paper VII)
van Driel, W., Balkowski, C., van Woerden, H. 1989, A&A, 218, 49 (paper VIII)
van Driel, W., van Woerden, H. 1989, A&A, 225, 317 (paper IX)
van Driel, W., van Woerden, H. 1991, A&A, 243, 71 (paper XI)
van Driel, W., de Jong, T. 1990, A&A, 227, 6
van Driel, W., van den Broek, A.C. 1991, A&A, 251, 431
van Woerden, H., van Driel, W., Schwarz, U.J. 1983, in IAU Symp. 100, Internal Kinematics and Dynamics of Galaxies, ed. E. Athanassoula, Reidel (Dordrecht), p. 99 (paper I)
Wainscoat, R.J., de Jong, T., Wesselius, P.R. 1987, A&A, 181, 225
Wardle, M., Knapp, G.R. 1986, AJ, 91, 23
Warner, P.J., Wright, M.C.H., Baldwin, J.E. 1973, MNRAS, 163, 163
Webster, B.L., Goss, W.M., Hawarden, T.G., Longmore, A.J., Mebold, U. 1979, MNRAS, 186, 31
Wesselius, P.R., Beintema, D.A., de Jonge, A.R.W., Jurriens, T.A., Kester, D.J.M., van Weerden, J., de Vries, J., Perault, M. 1985, IRAS-DAX Chopped Photometric Channel Explanatory Supplement, Lab. for Space Research, Groningen, The Netherlands
West, R.M., Surdej, J., Schuster, H.E., Muller, A.B., Laustsen, S., Borchkhadze, T.M. 1981, A&AS, 46, 57
Wevers, B.H.R.M., Appleton, P.N., Davies, R.D. 1984, A&A, 140, 125
Wevers, B.H.R.M., van der Kruit, P.C, Allen, R.J. 1986, A&AS, 66, 505
Williams, T.B., Schwarzschild, M. 1979, ApJ, 227, 56
Yoshizama, M., Wakamatsu, K. 1975, A&A, 44, 363